

# Action of Plane Frame Resting On Raft Foundation Subjected To Lateral Force

M.S.PADMANABAN

Lecturer(SG)/CIVIL

Central Polytechnic College, Chennai, Tamilnadu, India

## I. OBJECTIVE AND SCOPE

In the present investigation both interaction (INT) and non-interaction (N-INT) examinations were completed. In the non-cooperation examination, the powers and minutes got for the structure on an unfaltering base are connected on the pontoon - soil framework and examined autonomously. In the collaboration examination, all the three parts specifically soil, pontoon and superstructure are dissected as a solitary perfect unit and contrasted and non-collaboration investigation. A point by point parametric considers was led by shifting the relative stiffness of superstructure,  $k_{sb}$  and the relative stiffness of raft,  $k_{rs}$ . The relative stiffnesses  $K_{sb}$  and  $K_{rs}$  are resolved in light of the proposal of Brown *et al.* (1986), which are as per the following.

$$k_{sb} = \frac{E_s I^4}{m E_b I_b (1 - \nu_s^2)} \quad (1.1)$$

and

$$k_{rs} = \frac{16 E_r I_r (1 - \nu_s^2)}{\pi E_s L^4} \quad (1.2)$$

where  $m$  = Number of stories,  $E_b$  = Elastic modulus of shaft,  $E_s$  = Young's modulus of soil,  $E_r$  = Young's modulus of pontoon,  $I_b$  = Moment of Inertia of shaft,  $I_r$  = Moment of Inertia of pontoon,  $L$  = Length of the pontoon,  $l$  = Span of the shaft, and  $\nu_s$  = Poisson's proportion of soil.

The impact of these two parameters on the powers and minutes in superstructure and the pontoon were considered. Investigations are completed for the accompanying scopes of qualities:

$k_{sb} = 1$  to 100 and  $k_{rs} = 0.001$  to 0.01

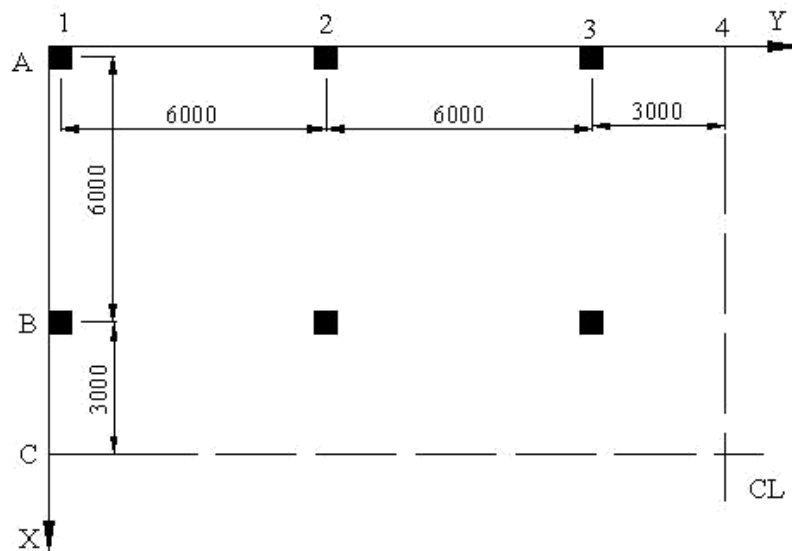
These reaches were chosen as they are of useful intrigue. The lower furthest reaches of  $k_{sb}$  speak to an expanding on the delicate or free store and the maximum furthest reaches of  $k_{sb}$  are a point past which there is a little collaboration impact. The lower furthest reaches of  $k_{rs}$  relate to an establishment of a least possible relative firmness and the maximum furthest reaches of  $k_{rs}$  speak to a semi unbending establishment. Accordingly, this investigation covers for the most part the semi adaptable conduct of the establishment framework. The different relative firmness was gotten for a consistent building solidness  $k_b$ , at that point choosing  $k_s$  to give the coveted estimation of  $k_{sb}$  lastly utilizing the chose estimation of  $k_s$  to decide  $k_r$  with the end goal that the coveted estimation of  $k_{rs}$  is acquired. The qualities for which examinations were performed are  $k_{rs} = 0.001, 0.005$  and  $0.01$  and  $k_{sb} = 15, 20, 30, 60$  and  $100$ . Thus, the objectives are

- i) To study the differential settlement for the interaction and non-interaction analysis.
- ii) To study the effect of relative stiffness
- iii) To study the influence of relative stiffness on the turn of the column base.
- iv) To study the influence of relative stiffness on the contact pressure.
- v) To study the relationship between the span, moments in the

Winkler model

## 2.1 PROBLEM STATEMENT

The arrangement of the quarter pontoon and the position of the segments of 3 bay 5 bay cove outlines are appeared in Figure 3.1.



(All dimensions are in mm)

Figure 2.1 Plan of quarter pontoon and segment position

The dividing between the segments is 6 m and the section stature between the floors is 3.5 m. An examination is done by accepting that the pontoon is set specifically on the sand bed. As a rule, sand is a non-homogeneous material, whose modulus changes with profundity. However the trial examination on the edge pontoon soil framework by including non-homogeneity appeared some effect on the aggregate settlement however just peripheral distinction on the differential settlement and additionally on the part powers. In this manner, the property of sand is thought to be uniform with profundity. In the investigation, the solidness of the divider and the chunk are excluded. The heap on the section counting self-weight and weight of the divider are considered and connected as consistently disseminated tacks on the bars. The geometric properties of the casing and the material properties embraced in the examination are exhibited in Table 2.1.

Table 2.1 Geometric and elastic properties of frame and raft and soil

Column size, m	Storey- 1,2,3	0.5 x 0.5	Span of beams, (l)	6 m
	Storey- 4, 5	0.4 x 0.4	Load on inner beams	35 kN/m
Beam size, m		0.3 x 0.6	Load on outer beams	28 kN/m
Floor height, m		3.5	Raft size, m	30 x 30 x 0.60
Modulus of concrete( $E_c$ )		$2.5 \times 10^7$ kPa	Poisson's ratio of concrete	0.15
Modulus of soil ( $E_s$ )		30 MPa	Poisson's ratio of soil	0.35

The complexities involved in the interaction analysis of the raft and the superstructure can be simplified to a larger extent if the finite element technique is used. The Finite element discretization of frame-raft-soil is shown in Figure 3.1.

### 3.1.1 Frame Model

The frame is modelled as an assemblage of beam elements (Beam4). Beam4 is a uniaxial element which has the capabilities of tension, compression, torsion and bending capabilities. This element has two nodes and six degrees of freedom at each node. They are translations in the nodal x, y, and z directions and rotations about the nodal x, y, and z directions. The joint between the columns and beams was assumed to be rigid.

### 3.1.2 Pontoon Foundation and Contact Element

The pontoon was demonstrated as a plate-bowing component (Shell93) with eight hubs having six degrees of opportunity at every hub. The minute per unit length of the pontoon is computed in the component co-ordinate framework. The interface qualities between the pontoon and the dirt are spoken to by the component Targe170 and Conta174.

### 3.1.3 Soil Model

The soil is dealt with as an isotropic, homogenous and versatile half space medium. For the direct examination, the underlying digression modulus ( $E_s$ ) and Poisson's proportion ( $\mu_s$ ) are the sources of info. The dirt medium underneath the pontoon was displayed utilizing the eight-hub block component (SOLID45) having three degrees of opportunity of interpretation in the x, y and z headings at every hub. Keeping in mind the end goal to discover the degree of the dirt locale to be utilized as a part of the investigation, numerous trial examinations are done. It is discovered that for the width and the thickness of the dirt medium more than 2.5 times the slightest width of the pontoon establishment demonstrates an insignificant effect on the settlement and the contact weight. The vertical interpretation is captured at the base limit while the sidelong interpretation is captured at the vertical limit. Fine works with angle proportion 1.0 are created near the pontoon while networks created far from the pontoon region are made coarser continuously.

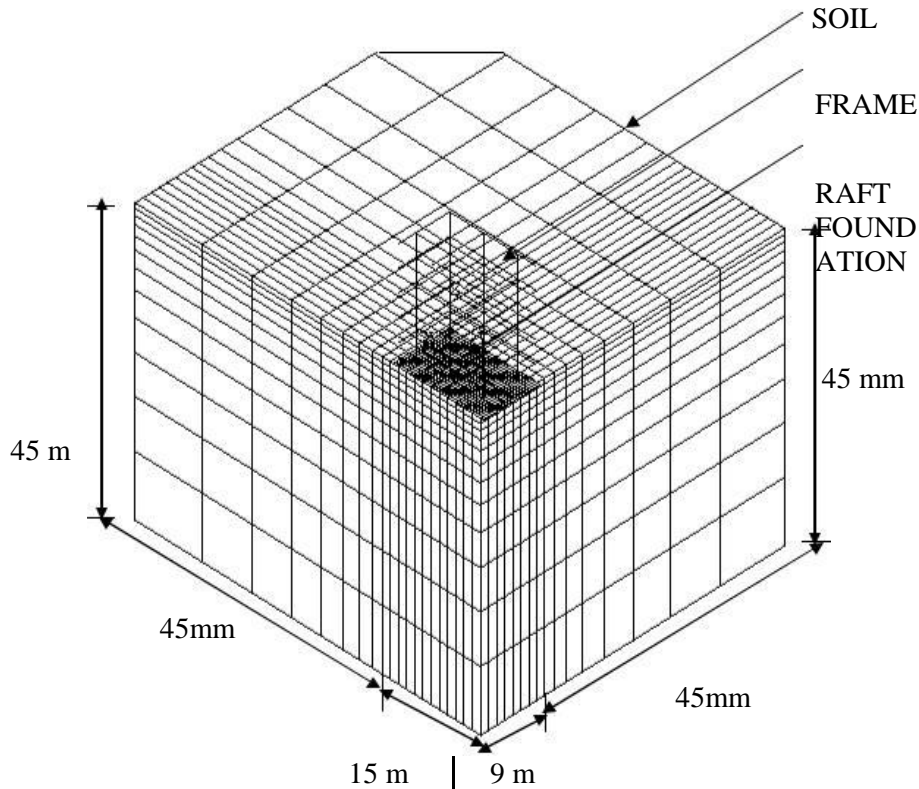


Figure 2.3 Frame-raft-soil and element discretization (Quarter model)

A rectangular raft of 18 m x 30 m supporting 24 columns spaced at 6 m centre to centre on both the directions was analyzed for the linear behaviour of the soil. The results of the analyses are presented and discussed.

### 3.1 SETTLEMENT OF THE RAFT

The settlement ( $w$ ) of the pontoon decided from the non-communication (N-INT) and the communication (INT) examinations are standardized with separating between the segments, ( $l$ ) and introduced in figure 4.1 for the relative solidness of structure  $k_{sb} = 20$  and the pontoon  $k_{rs} = 0.001$ . In this figure, the standardized settlement,  $w/l$  ( $w$  = settlement,  $l$  = traverse) of the pontoon along the area A1-A4 and B1-B4 are thought about. In both the areas, the settlement at the focal point of the pontoon is higher than the settlement at the edge independent of the techniques embraced. The distinction in the settlement between the techniques is less at both the longitudinal segments and the differential settlement is diminished because of the connection. The diminishments in the differential settlement at these segments are 21% and 18% individually. With a specific end goal to comprehend the impact of  $k_{rs}$  on the settlement, the variety of the standardized settlement along the segment A1-A4 is exhibited in figure 4.2 for an arrangement of  $k_{rs}$  and  $k_{sb}$  esteems. The settlement of the pontoon is higher for bring down  $k_{sb}$  esteem, regardless of the  $k_{rs}$  esteems. For the  $k_{sb}$  esteem of 15, the most extreme settlement along the segment A1-A4 is around 0.70 % of the traverse ( $l$ ). In spite of the fact that there isn't much distinction in the settlement between the  $k_{rs}$  estimations of 0.001 and 0.01, the differential settlement

is less by 16% for the  $k_{rs}$  estimation of 0.01. This demonstrates the increment in the pontoon thickness has just a peripheral impact on the settlement. In any case, the increment in the  $k_{sb}$  impacts the settlement which is obvious from the considerable abatement in the settlement. The lessening in the differential settlement is 20%, which again demonstrates that the modulus of the dirt has more impact than the thickness of the pontoon in decreasing both the aggregate and the differential settlement of the establishment soil framework.

Figure 4.3 delineates the variety of the aggregate settlement with  $k_{sb}$  at the segment focuses. The settlement at the segment point is lessened obviously for the  $k_{sb}$  esteems in the vicinity of 15 and 60 and for the  $k_{sb}$  esteems more than 60; the decrease in the settlement is immaterial. In addition, the size of the settlement was less ( $< 10$  mm) for higher  $k_{sb}$  esteems ( $>60$ ) independent of the segment areas for the power of the heap considered in this examination. Figure 4.4 demonstrates the variety of the standardized settlement,  $w/l$  along the area B1-B4 for different  $k_{sb}$  esteems. In general, the settlement at the focal point of the pontoon is higher than that at the edge independent of the  $k_{sb}$  esteem. Notwithstanding, the settlement along the area B1-B4 diminishes obviously with the increment in  $k_{sb}$  esteem and the distinction in the settlement between the focuses B1 and B4 was observed to be less. The most extreme decrease in the differential settlement between  $k_{sb}=15$  and 100 along this segment is 81% for  $k_{rs} = 0.001$  and the most extreme lessening in the differential settlement between  $k_{sb} = 15$  and 100 along this segment is 82% for  $k_{rs} = 0.01$ . in the differential and the aggregate settlement along the transverse segment A3-C3 is 86% for the increment in  $k_{sb}$  esteem from 15 to 100 and  $k_{rs} = 0.001$ .

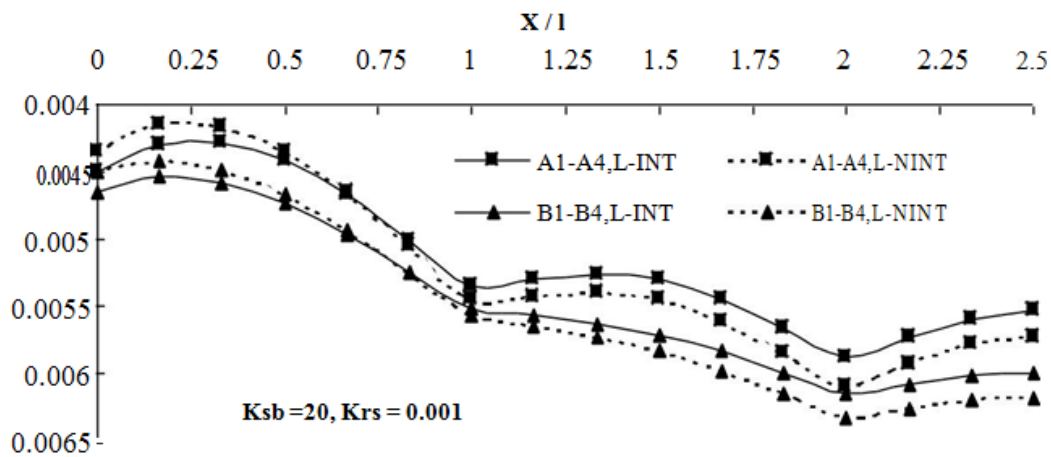


Figure 3.1 Normalized settlements along A1-A4 and B1-B4

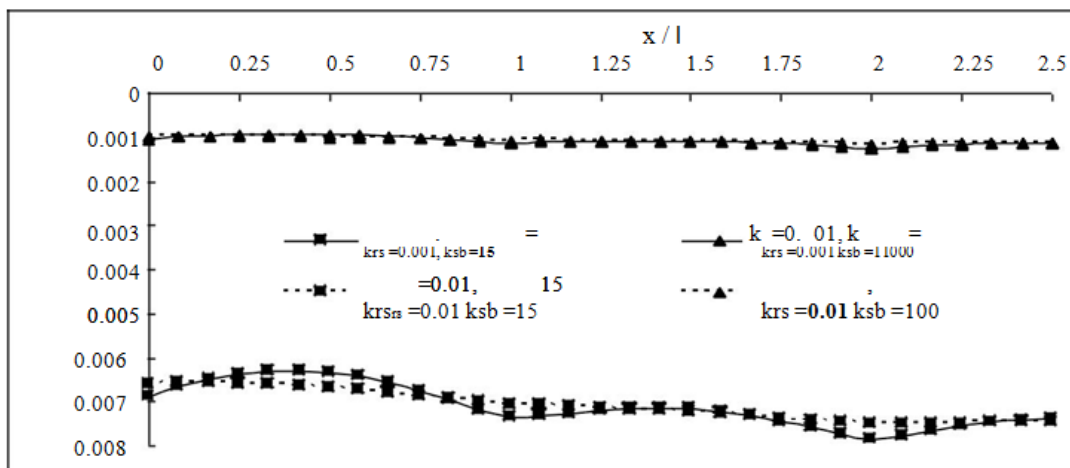


Figure 3.2 Normalized settlements along the section A1-A4 of the raft

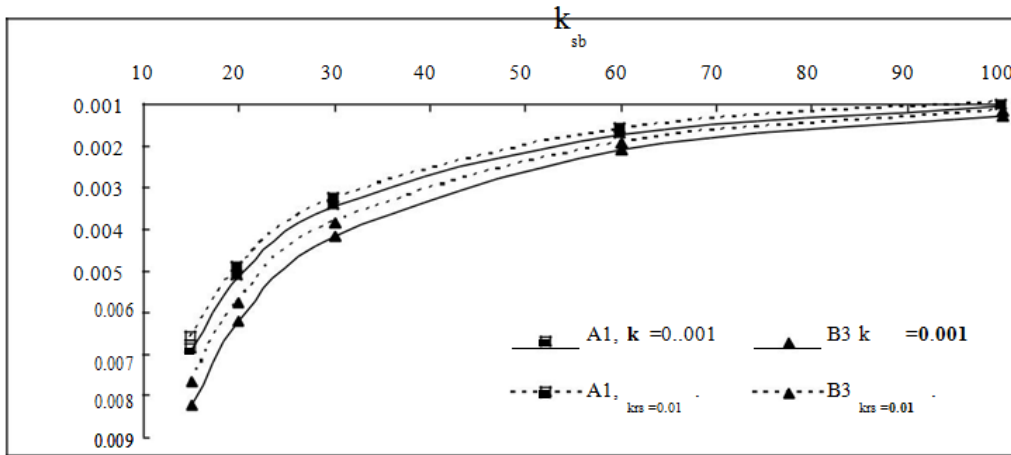


Figure 3.3 Variation of total settlement with  $k_{sb}$  in the raft at the column points

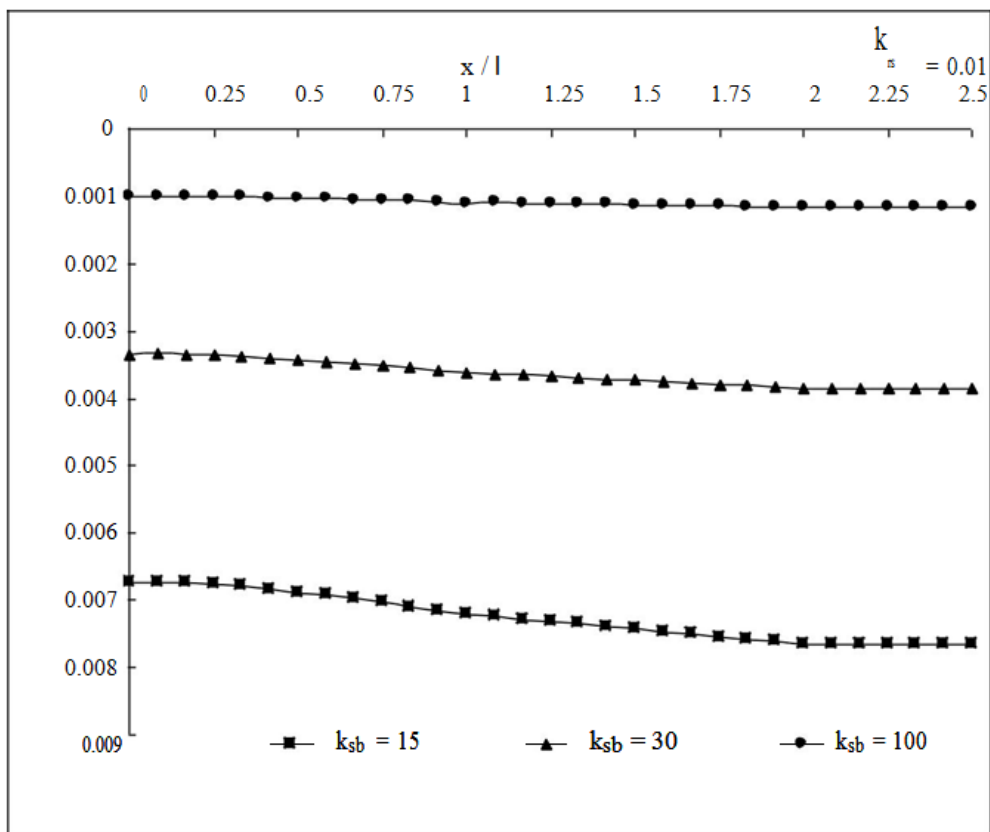


Figure 3.4 Normalized settlements along B1-B4 for various values of  $k_{sb}$

### 3.2 HORIZONTAL RELOCATION OF THE RAFT

The deviation of the horizontal relocation of the raft beneath the column along  $x$  direction for  $k_{rs} = 0.001$  is shown in Figure 4.5. The columns which are placed by the side of the border of the raft (A1, A2 and A3) dislocate laterally along the positive direction of  $x$ -axis, while the inner columns (B1, B2 and B3) move in the opposite direction and towards the outer columns. But the relocations of the inner columns are much smaller than those of the outer columns which are 5% to 20% of the outer column relocations. The enhancement in firmness factors  $k_{sb}$  and  $k_{rs}$ , reduces the lateral relocation of the columns.

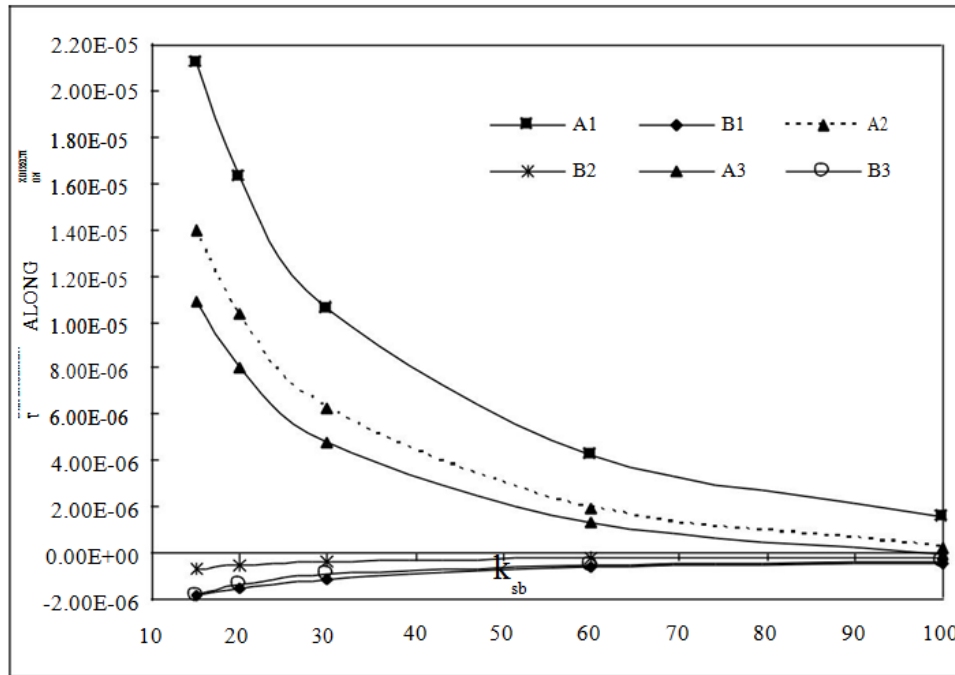


Figure 3.5 Variation of lateral displacement ( $U_x$ ) in the pontoon under the section

### 3.3 TURN OF COLUMN BASES

Figure 4.6 demonstrates the turn of the section bases about x y hub for different  $k_{sb}$  esteems. The pivot of the section base appeared in the figure is the slant of the disfigured state of the pontoon by then. For the most part, at the corner and the edge of the pontoon the incline is greatest. The pivot of the external lines of the segments about y hub (A1, A2 and A3) is around 350% higher than the internal line sections (B1, B2 and B3). Be that as it may, they pivot the other way. The distinction in the turn among the sections of the internal or the external column is minimal especially if the  $k_{sb}$  esteems are higher than 60. The expansion in  $k_{sb}$ , brings about the diminishment in the pivot of the considerable number of segments, particularly segment A1 has the most extreme diminishment. The expansion in the unbending nature of the pontoon diminishes the turnabout x and y headings and are lessened by 98% what's more, 83% individually for the expansion in estimation of  $k_{rs}$  from 0.001 to 0.01. Among the two factors  $k_{sb}$  and  $k_{rs}$ , the  $k_{rs}$  has more effect on the turn of the pontoon chunk.

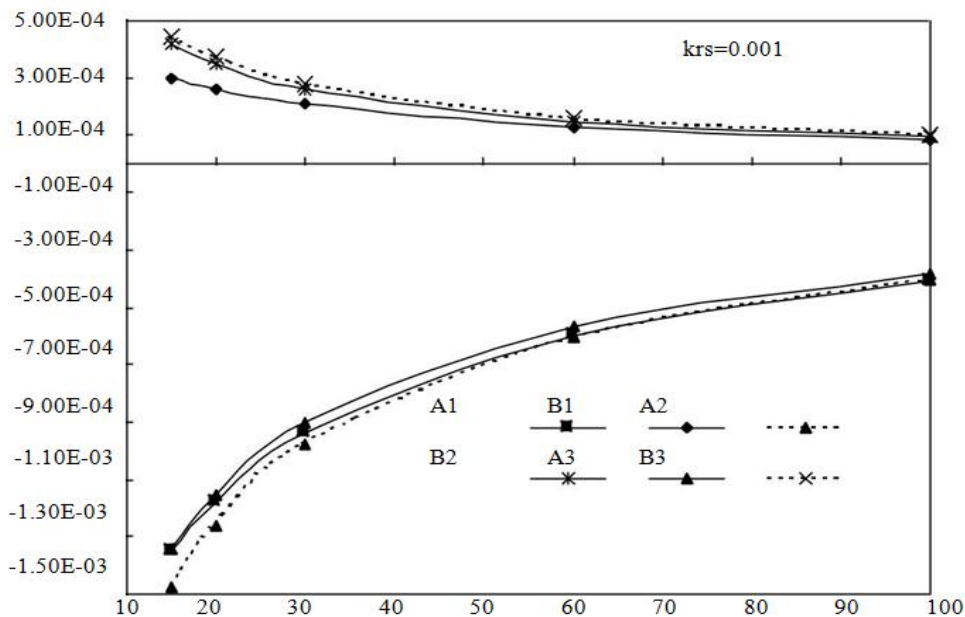


Figure 3.6 Variation of rotation in the raft beneath the Columns



### 3.4 CONTACT PRESSURE UNDERNEATH THE RAFT

The contact weight circulation is exhibited in figure 4.7 for the longitudinal areas A1-A4 and B1-B4 of the pontoon. It is seen from the assumption that the contact weights at the edges are higher than that at the middle. In any case, the size of the contact weight is most extreme at the corner of the pontoon. In the corners, the convergence of the contact weight is around 11 times the normal weight, ( $q = \text{add up to vertical load/region of the pontoon}$ ). Essentially, at the edge (ie along the fringe) the same is 4.5 times the  $q$  esteem. Be that as it may, they act over an extremely littler zone and radically make tracks in an opposite direction from the edge and the corner purposes of the pontoon. The contact weight at the inside piece of the pontoon is uniform with the extent and found to change between  $0.7q$  and  $1.0q$ . A common conveyance of the contact weight of the pontoon at the inside and the corner is appeared for different  $k_{rs}$  and  $k_{sb}$  blends at the middle and the side of the pontoon. For the estimations of  $k_{rs}$  (0.001 and 0.01) and  $k_{sb}$  (15 and 100) appeared in the figure, the contact weight at the inside piece of the pontoon along B1-B4 is 0.8 times the normal weight. The impact of  $k_{sb}$  on the contact weight is practically nil. Be that as it may, the contact weight diminishes with the increment in  $k_{rs}$  especially at the segment focuses and the conveyance turns out to be more uniform over most parts of the pontoon aside from at the edges and the corners. The example of the contact weight got from the FEM investigation demonstrated a higher edge weight and it diminishes towards the focal point of the pontoon. Regardless of the  $k_{sb}$  and  $k_{rs}$  esteems, the example of the contact weight dissemination is practically the same along any given segment of the pontoon. In any case, there is some adjustment in the extent of the contact weight. This example is especially indistinguishable to that of the conveyance revealed somewhere else by the prior scientists utilizing conditions of the flexible hypothesis and FEM investigation. A comparative pattern is seen at the section areas A2 and B2. At the section A2, the contact weight is considerably higher than the segment B2 regardless of the relative solidness of the pontoon ( $k_{rs}$ ). As expressed before the contact weight is autonomous of  $k_{sb}$  esteems however it diminishes with the expansion in  $k_{rs}$ . From the above exchange the modulus of the dirt ( ie  $k_{sb}$  ) has less impact on the contact weight dispersion.

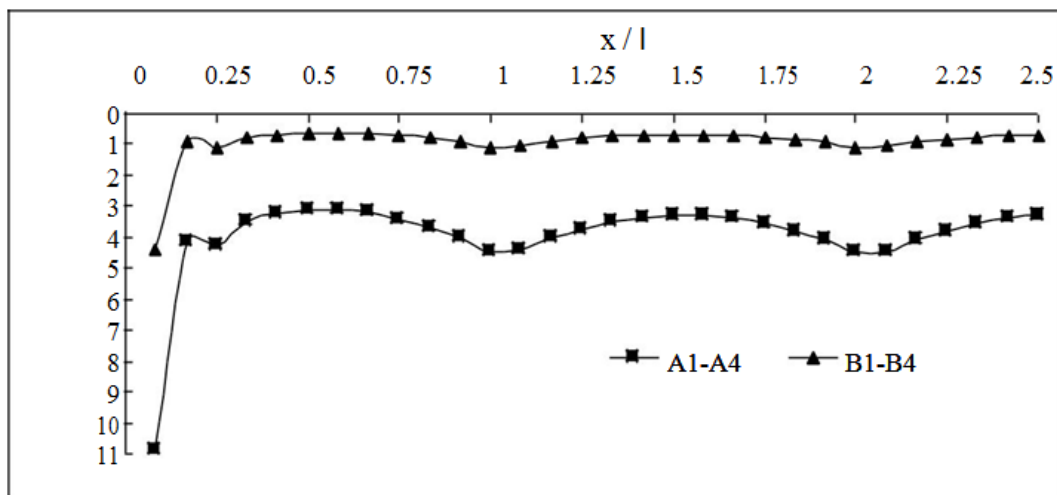


Figure34.7 Contact pressure distributions along A1-A4 and B1-B4

A typical distribution of the contact pressure of the raft at the centre and the corner is shown in Figure 4.8 for various  $k_{rs}$  and  $k_{sb}$  combinations at the centre and the corner of the raft. For the values of  $k_{rs}$  (0.001 and 0.01) and  $k_{sb}$  (15 and 100) shown in the figure, the contact pressure at the centre part of the raft along B1-B4 is 0.8 times the average pressure. The influence of  $k_{sb}$  on the contact pressure is almost negligible. But the contact pressure decreases with the increase in  $k_{rs}$  particularly at the column points and the distribution becomes more uniform over most parts of the raft except at the edges and the corners. The pattern of the contact pressure obtained from the FEM analysis showed a higher edge pressure and it decreases towards the centre of the raft. Irrespective of the  $k_{sb}$  and  $k_{rs}$  values, the pattern of the contact pressure distribution is almost the same along any given section of the raft. However, there is some change in the magnitude of the contact pressure. This pattern is very much identical to that of the distribution reported elsewhere by the earlier researchers using equations of the elastic theory and FEM analysis. A similar trend is seen at the column locations A2 and B2. At the column A2, the contact pressure is much higher than the column B2 irrespective of the relative stiffness of the raft ( $k_{rs}$ ). As stated earlier the contact pressure is independent of  $k_{sb}$  values but it decreases with the increase in  $k_{rs}$ . From the above discussion the modulus of the soil ( ie  $k_{sb}$  ) has less influence on the contact pressure distribution.

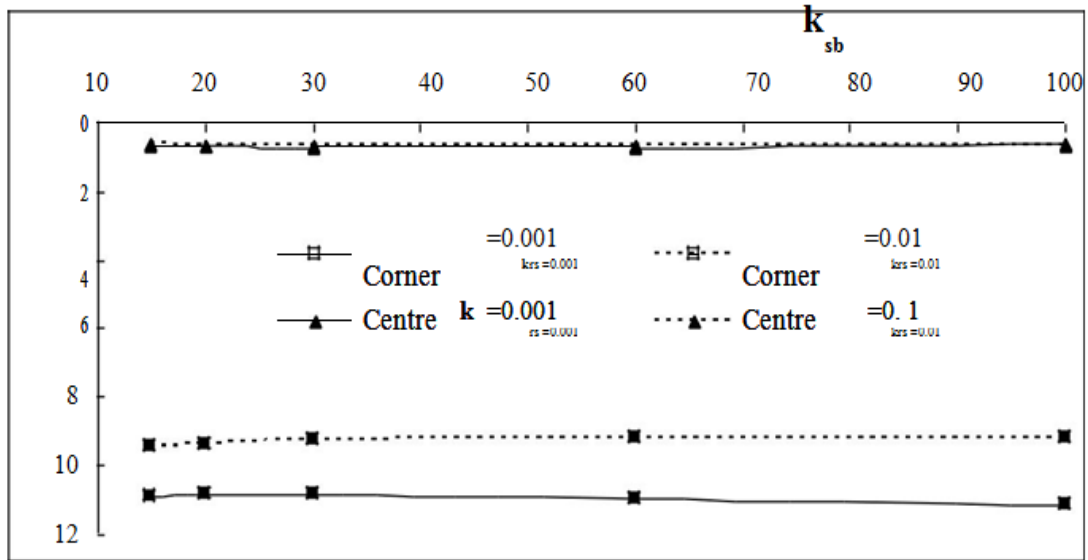


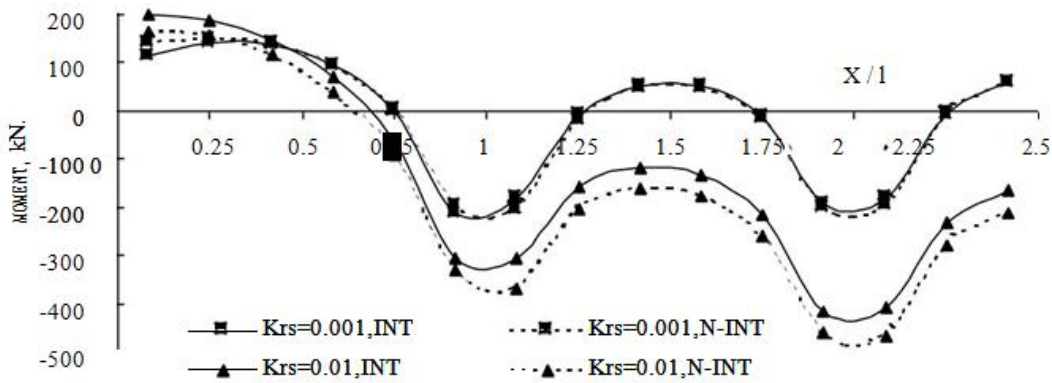
Figure 3.8 Distribution of contact pressure at corner and centre along B1-B4 for  $k_{rs} = 0.001$  and  $0.01$

From the results of the variation of the thickness of the foundation the variation of  $U_{zmax}$  is Compression load,  $\sigma_{max}$  is the Contact stress and  $M_{max}$  is Moment are denoted in above table. The load acting on the foundation is uniform and has a value of  $100\text{kN/m}^2$ . In the additional plate and SM model the average of the contact stress is not equal to the external force acting on the foundation surface. Part of the stress will be taken by the soil around the foundation slab, because the slab is very thick (1.25m). The amount of stress that disappears cannot be seen in the final calculation results. This can cause complications for designers because they cannot approximate the amount of stress that is transferred to neighbouring structures.

### 3.6 BENDING MOMENT IN THE RAFT

The bending moments arrived at from the non-interaction and the interaction analyses are compared in Figure 4.25 for the  $k_{rs}$  values of 0.001 and 0.01 with  $k_{sb} = 20$ . For the  $k_{rs} = 0.01$  the bending moment along the section B1-B4 is appreciably higher than  $k_{rs} = 0.001$  for both the interaction and the non-interaction conditions. A similar trend is seen in all other sections of the raft, which indicates that the stiffness of the raft has a significant influence on the bending moment. Further, the difference in the bending moment between the two methods is also higher for higher  $k_{rs}$  (0.01) value. The maximum difference is 12% for the conditions of the problem analysed. The support moments  $M_x$  and  $M_y$  in the raft at the location of all the columns are compared in Table 2 for the various  $k_{rs}$  and  $k_{sb}$  values. For the raft-frame (3 bays x 5 bays, 5 Storey) system analysed, the raft moments  $M_x$  and  $M_y$  are the maximum at a given column location for the  $k_{rs} = 0.01$  irrespective of the  $k_{sb}$  values. Among the columns,  $M_x$  and  $M_y$  are maximum and minimum for the column A3 and B1 respectively irrespective of  $k_{sb}$  values. However, for a given  $k_{sb}$  the most affected locations are the column points along the edges (A1, B1 for  $M_x$  and A1, A2 and A3 for  $M_y$ ). Both  $M_x$  and  $M_y$  values changes significantly in these columns due to the increase in  $k_{rs}$  values from 0.001 to 0.01. The least affected locations are the column points B2 and B3 irrespective of  $k_{rs}$  and  $k_{sb}$  values. Further, the difference in the moment between  $M_x$  and  $M_y$  is more in the locations of the edge columns. The variation of the span moment along the length and the width of the raft are summarized in Table 4.2. For a given  $k_{sb}$ , the span moment decreases at any section with the increase in  $k_{rs}$  except at the end spans of all the sections. In the end spans the increase in the moment due to the increase in  $k_{rs}$  is found to vary from 6% to 33% and the maximum increase is for the lowest  $k_{sb}$  value. However, the variation in the moment with the increase in  $k_{sb}$  is marginal, particularly for  $k_{rs} = 0.001$ . But for the value of  $k_{rs} = 0.01$  the variation is more than 50% at most of the locations.





- Figure 3.7 Variation in bending moment along B1-B4 of raft ( $k_{sb} = 20$ )

Table 3.2 Bending moment in the raft at the column bases

Column	$k_{rs}$	Moment ( $M_x$ ) kNm			Column	$k_{rs}$	Moment ( $M_y$ ) kNm		
		$k_{sb}=20$	$k_{sb}=60$	$k_{sb}=100$			$k_{sb}=20$	$k_{sb}=60$	$k_{sb}=100$
A1	0.001	8	122	164	A1	0.001	-2	114	150
	0.01	280	280	277		0.01	233	255	260
A2	0.001	-439	-402	-383	A2	0.001	32	113	142
	0.01	-438	-385	-361		0.01	163	197	207
A3	0.001	-391	-380	-370	A3	0.001	49	121	147
	0.01	-516	-493	-475		0.01	171	199	208
B1	0.001	51	124	150	B1	0.001	-426	-402	-387
	0.01	216	221	223		0.01	-446	-405	-384
B2	0.001	-334	-314	-307	B2	0.001	-335	-322	-318
	0.01	-361	-358	-357		0.01	-377	-379	-379
B3	0.001	-308	-312	-312	B3	0.001	-322	-320	-319
	0.01	-465	-482	-485		0.01	-389	-393	-393

Table 3.3: Bending moment in the raft at the span

Span	$k_{rs}$	Span moment ( $M_x$ ) kNm			Span	$k_{rs}$	Span moment ( $M_y$ ) kNm		
		$k_{sb}=20$	$k_{sb}=60$	$k_{sb}=100$			$k_{sb}=20$	$k_{sb}=60$	$k_{sb}=100$
A1- A2	0.001	235	236	235	A1-B1	0.001	239	243	244
	0.01	290	264	253		0.01	289	269	260
A2- A3	0.001	143	139	136	A2-B2	0.001	167	179	185
	0.01	50	20	14		0.01	208	222	230
B1- B2	0.001	170	184	190	A3-B3	0.001	157	173	180
	0.01	230	238	245					
B2- B3	0.001	58	57	57		0.01	193	211	220
	0.01	-26	-39	-41					

In previous paper, SOLID 45(linear elements) was chosen for Soil arrangement. If we still use linear elements then, there will not be correct discretization of elements. So, in this model, Quadratic elements were chosen for Soil arrangement.

#### IV. CONCLUSION

##### 4.1 Raft-Soil Interaction

From the interaction and the non-interaction analyses of the soil- raft frame system, the following important conclusions are drawn.

I. From investigation done between the two analyses, it has been observed that less total and differential settlements are obtained in interaction analysis than the non-interaction analysis did between the two parameters namely relative stiffness of the raft  $k_{rs}$  and relative stiffness of the structure  $k_{sb}$ .  $k_{sb}$  has a significant influence on both the settlements indicating that the modulus of the soil plays major role in the performance of the raft.

II. There is reduction in the rotation of the columns due to increase in  $k_{sb}$ , particularly the corner column has the maximum reduction.

III. The effect of  $k_{sb}$  on the contact pressure is almost negligible. The contact pressure at the middle part of the raft is observed to vary between  $1.4q$  ( $q$ =average pressure) and  $0.9q$ . The contact pressure is inversely proportional to thickness of the raft. The distribution of contact pressure beneath the footings is non uniform. It is less near the middle and very large near the edges, as it occurs below rigid footings on elastic continuum. These maximum values of contact pressures are of unequal in magnitude at the outer and inner edges. This may be one of the causes for significant change of stresses from integrated analysis, when matched with separate analysis. The other cause may be the differential settlement among footings.

IV. From the investigations, the moments in the raft and the end span is directly proportional to the  $k_{sb}$  value, whereas  $k_{rs}$  changes the moment beneath the interior columns as well as the span moment in the interior panels of the raft.

### REFERENCES

- [1]. ABAQUS 2005, Hibbitt, karlsson and Sorensen. Inc., Version 6.5.
- [2]. Ahmad, S & Mamoon, SM 1991, 'Seismic Response of Floating Pilesto Obliquely Incident Waves', Proc. of 2nd International Conference on Recent Advances in Geotechnical Earthquake Engineering and Soil Dynamics, St. Louis, MO., University of Missouri-Rolla Publication, pp. 805-814.
- [3]. Allen D.N. and Severn R.T. (1961) 'The stresses in foundation rafts', Proc. ICE., Vol.20, pp.293-304.
- [4]. Bardet, JP 1989, 'Prediction of deformations of Hostun and Reid Bedford sands with a simple bounding plasticity model', in Constitutive Equations for Granular Non-cohesive Soils, A. Saada and G. Bianchini Eds., Balkema, pp. 131-148.
- [5]. Bentley, KJ & Naggar, MHEI 2000, 'Numerical analysis of kinematic Response of single piles', Canadian Geotechnical Journal, vol. 37, pp. 1368-1382.
- [6]. Borja, RI & Amies, AP 1994, 'Mutiaxial Cyclic Plasticity Model for Clays', Journal of Geotechnical Engineering, ASCE, vol. 120, no. 6, pp. 1051-1070.
- [7]. Borja, RI, Chao, HY, Montans, FJ & Lin, CH 1999, 'Nonlinear Ground response at Lotung LSST site.' Journal of Geotechnical and Geoenvironmental Engineering, ASCE, vol. 125, pp. 187-197.
- [8]. Boussinesq, M. J. (1885), "Application des potentiels a l'etude de l'equilibre et du mouvement des solides elastiques, principalement au calcul des deformations et des pressions que produisent, dans ces solides, des efforts quelconques exercees sur une petite partie de leur surface ou de leur interieur: Memoire suivi de notes etendues sur divers points de physique mathematique et d'analyse," GauthierVillars, Paris, pp. 722.
- [9]. Brown P.T. and Yu Si K.R. (1986) 'Load Sequence and Structure-foundation-Interaction', Journal of Structural Engineering, Vol. 112, No. 3, pp. 481-488. - 877